NOTES AND CORRESPONDENCE

Momentum Flux from Wind to Aqueous Flows at Various Wind Velocities and Fetches

JIN WU

Air–Sea Interaction Laboratory, College of Marine Studies, University of Delaware, Lewes, Delaware

21 April 1987 and 10 July 1987

ABSTRACT

The fraction of wind stress consumed in driving aqueous flows has been estimated for various nondimensional fetches, derived from the wind velocity, fetch, and gravitational acceleration. The fraction is shown to vary with both fetch and wind velocity; at all fetches it is smaller at lower wind velocities, and for most winds it is smaller at shorter fetches.

1. Introduction

In order to understand physical processes of air–sea interaction, we must first quantify the partition of momentum flux from wind into waves and currents. The fraction of wind stress transferred directly to long waves was evaluated by Hasselmann et al. (1973), Phillips (1977), Snyder et al. (1981), and Mitsuyasu (1985); wide discrepancies, however, exist among their results. Moreover, its variations with wind velocity and fetch have not been considered in these studies. In the meantime, the total wind stress has generally been used in oceanic models to drive aqueous flows, implying that the shear stress is continuous across the air–sea interface.

A correlation has been established between the wind-stress coefficient and nondimensional fetch derived from boundary-layer parameters: fetch and wind velocity (Wu, 1985). In addition, the wave age is shown to have a unique relationship with the nondimensional fetch, and therefore serves as an alternate parameter of the latter. Using these results along with those of Hasselmann et al. (1973) on waves, we have estimated the partition of wind stress in producing waves and aqueous flows at various fetches and wind velocities.

2. Estimate of direct momentum flux to waves

a. Wind-stress coefficient

On the basis of the logarithmic wind profile within the atmospheric surface layer and the Charnock equation describing the growth of roughness length with wind velocity, an expression for determining wind-stress coefficients under different wind velocities at various fetches was derived (Wu, 1985):

$$C_z^{1/2} = \kappa/\ln[(0.14/C_z)(gL/U_z^2)]^{2/3}. \qquad (1)$$

Herein the wind-stress coefficient C_z is related to wind velocity U_z measured at anemometer height Z above the mean water surface, $\kappa = 0.4$ the von Kármán universal constant, g the gravitational acceleration, and L the fetch; this variation is illustrated by a dashed line in Fig. 1. Increasing with the surface-layer thickness, the anemometer height for various fetches and wind velocities, to be sufficiently away from the water surface to avoid wave-induced motions and yet still within the constant-flux layer where the logarithmic profile prevails, has been suggested as (Wu, 1971):

$$Z = 7.35 \times 10^{-7}R^{2/3}\ (\text{m}), \quad R < 5 \times 10^{10} \qquad (2)$$

where $R = U_zL/\nu$ is the fetch Reynolds number, with ν being the kinematic viscosity of air. For the open sea with $R > 5 \times 10^{10}$, the anemometer height has customarily been kept at 10 m.

Field results obtained at finite fetches, however, are still referred to the wind velocity measured at 10 m above the mean water surface. The wind-stress coefficient C_z defined with U_z was therefore converted to C_{10} defined with the corresponding wind velocity (U_{10}) at the 10-m elevation; the logarithmic wind profile, (1), and the formula $C_{10} = (0.8 + 0.065\ U_{10}) \times 10^{-3}$ suggested by Wu (1980) were used in the conversion. The results for C_{10} under three wind velocities $U_{10} = 5$, 10 and 15 m s^{-1} are presented as solid lines in Fig. 1. Trends of two sets of results, C_z versus gL/U_z^2 and C_{10} versus gL/U_{10}^2, are rather different. First of all, there is no longer a unique variation between the wind-stress coefficient and nondimensional fetch when U_z is replaced by U_{10} in both parameters; each line now illustrates the variation of the wind-stress coefficient with fetch at only a given U_{10}. Much more gradual variations

Corresponding author address: Dr. Jin Wu, Air–Sea Interaction Laboratory, College of Marine Studies, University of Delaware, Lewes, DE 19958.

© 1988 American Meteorological Society

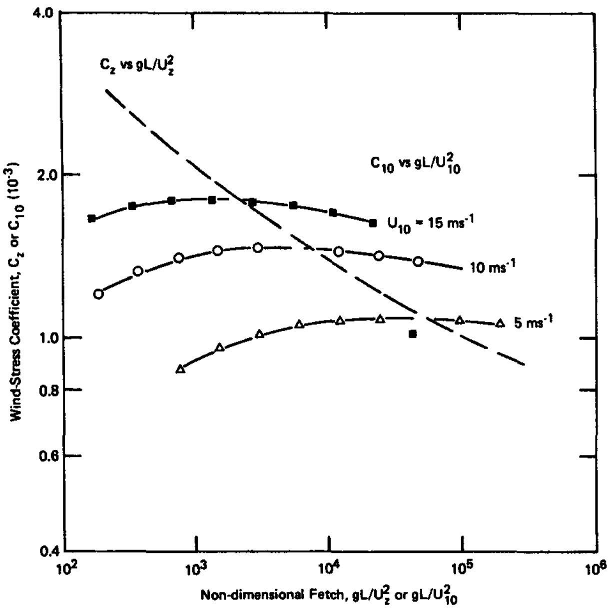

FIG. 1. Variations of wind-stress coefficients with nondimensional fetches.

of C_{10} with gL/U_{10}^2 are of course the artifact of using the wind velocity at nonequivalent elevations; in other words, the "standard" anemometer height of 10 m is too high for short fetches and too low for long fetches in the atmospheric surface layer that develops continuously with fetch.

b. Wave-drag coefficient

1) FORMULATION

The direct momentum flux to waves from a steady wind is due to the growth of waves in the wind direction (Stewart, 1961); this is the so-called wave drag. Wave components over a wide range of the spectrum receive direct momentum flux from the wind. Experimental evidence cited by Phillips (1977) indicates that the flux not lost immediately to breaking is mainly to wave components in the range from the spectral peak to where $c/u_* = 5$, in which c is the phase velocity of wave component and u_* the friction velocity of wind. The momentum flux communicated to these waves, τ_w, can be estimated from (Phillips, 1977):

$$\tau_w = \overline{p\nabla\zeta} = 2.5 \times 10^{-2}\rho_a U_{10}^2\overline{s^2} \quad (3)$$

where p is the pressure, $\nabla\zeta$ the surface slope, ρ_a the air density, and $\overline{s^2}$ the mean-square slope in the wind direction associated with wave components in the range previously mentioned. The mean-square slope can be related to the wavenumber spectrum $\psi(\mathbf{k})$ as

$$\overline{s^2} = \int k^2\psi(\mathbf{k})d\mathbf{k}, \quad \psi(\mathbf{k}) = (B/\pi)k^{-4} \quad (4)$$

where $\mathbf{k}$ and k are wavenumber vector and scalar, respectively, and B is the coefficient of the wavenumber spectrum; note that we deal primarily with waves in the gravity range. Recently, the wavenumber spectrum was suggested to follow $\psi(\mathbf{k}) \sim k^{-7/2}$ near the spectral peak (Phillips, 1985), but the high wavenumber part still follows k^{-4} (Leykin and Rozenberg, 1984); the latter part is the major contributor to the mean-square slope.

2) INTEGRATION LIMITS

Field results on the wave frequency at the spectral peak, f_m, were compiled by Hasselmann et al. (1973) along with their own results from the North Sea Wave Project (reproduced in Fig. 2a). Taking also into account the laboratory data obtained at much smaller nondimensional fetches, but not reproduced here, Hasselmann et al. suggested $f_mU_{10}/g = 3.5[gL/U_{10}^2]^{-0.33}$, shown as a dashed line in Fig. 2a. The line fails to represent the trend of field data, as laboratory and field results were seen in their original presentation to follow distinctly different variations. This is not unexpected, as wind and wave conditions in laboratory tanks may not be dynamically similar to those in the field in the sense that wave structures at extremely short fetches existing in laboratory tanks can be characterized by the nondimensional fetch. Consequently, we choose to use only the field data, which are seen to be represented much more closely by the solid line. The latter can be expressed as

$$f_mU_{10}/g = 2.25[gL/U_{10}^2]^{-0.25} \quad (5)$$

or

$$c_0/U_{10} = 0.0707[gL/U_{10}^2]^{0.25} \quad (6)$$

in which c_0 is the phase velocity of the wave component at the spectral peak, and the dispersion relationship of deep-water waves, $c_0 = g/2\pi f_m$, was substituted. The lower limit of integration, c_0, at various nondimensional fetches can then be obtained from (6), while the upper limit of the integration, $5u_*$, can be obtained from the results shown in Fig. 1.

3) SPECTRAL COEFFICIENT

The form of the wave spectrum at high frequencies, the equilibrium spectrum mentioned earlier, was proposed by Phillips (1958) as

$$\phi(n) = \beta g^2n^{-5} \quad (7)$$

where β is the coefficient of the wave-frequency spectrum. Earlier field results of β were also compiled by Hasselmann et al. (1973) along with their own results (Fig. 2b). Again combining laboratory and field data, they suggested that the spectral coefficient varied with the nondimensional fetch as $\beta = 0.076[gL/U_{10}^2]^{-0.22}$, shown as a dashed line in the figure. As discussed earlier, laboratory and field data again have distinctly different trends; the field results alone are seen to follow more closely the solid line expressed as

$$\beta = 0.116[gL/U_{10}^2]^{-0.3}. \quad (8)$$

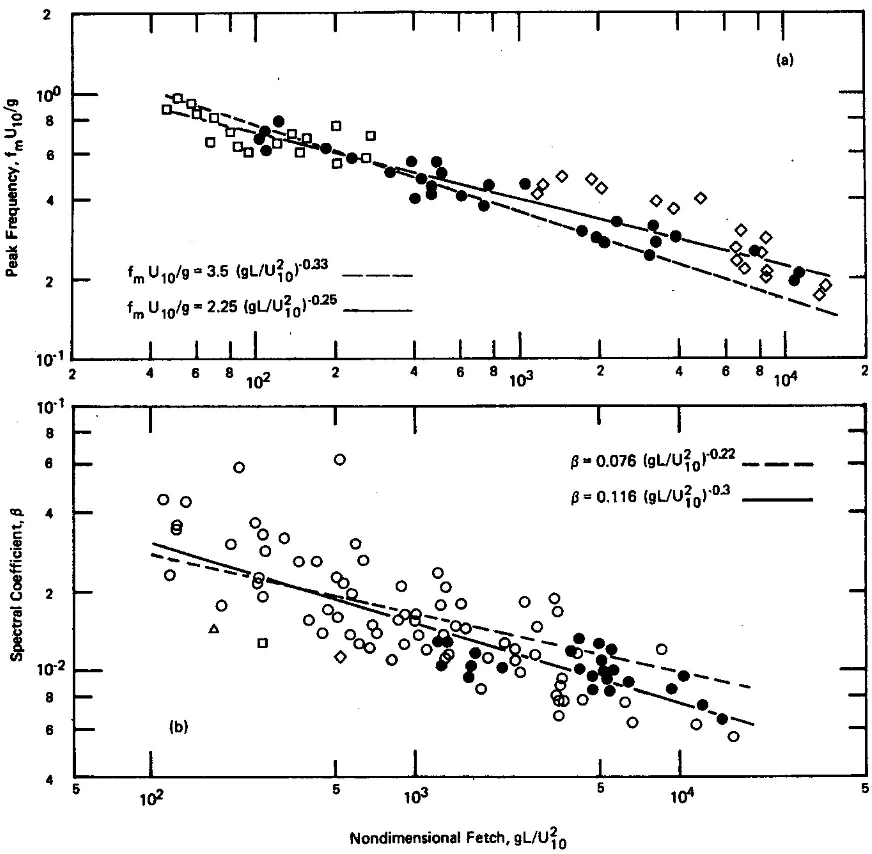

FIG. 2. Variations of peak frequency and spectral coefficient with nondimensional fetch. The data are from Burling (1959), □; Hicks (1960), △; Kinsman (1965); ◇; Liu (1971), ●; and Hasselmann et al. (1973), ○.

The approximate interrelation between coefficients of frequency and wavenumber spectra is $\beta = 2B$ (Phillips, 1977); consequently, we have

$$B = 0.058[gL/U_{10}^2]^{-0.3}. \tag{9}$$

As discussed earlier, the equilibrium spectrum was modified recently by Phillips (1985) to have a different form $\phi(n) \sim n^{-4}$ primarily near the spectral peak, and to remain at n^{-5} at high frequencies. In any event, we are interested in neither the spectrum itself nor finer spectrally resolved results, but in estimating the energy contained over a major portion of the wave system. The modification should not affect this estimate by adopting (7), deduced from the best fit to the measured spectrum. The use of (7) is also due to practical reasons, as the reported data on variations of the spectral coefficient of modified spectrum with the nondimensional fetch are not as comprehensive as those presented in Fig. 2b.

4) ESTIMATES

The coefficient of wave drag can be obtained from (3) and (4) as

$$C_v = \tau_w/\rho_a U_{10}^2 = 2.5 \times 10^{-2} B \ln(k_c/k_0) \tag{10}$$

where k_c and k_0 are the wavenumbers corresponding to $c = 5u_*$ and c_0, respectively. Substituting B, k_c and k_0 into the above expression, we have

$$C_v = 1.45 \times 10^{-3}[gL/U_{10}^2]^{-0.3} \ln(c_0/5u_*)^2. \tag{11}$$

The results obtained at $U_{10} = 5$, 10, 15, and 20 m s^{-1} are shown in Fig. 3a. It is interesting to see that all lines converge as the nondimensional fetch increases.

The variation of the ratio between the wave drag and wind stress with the nondimensional fetch, calculated from the results shown in Figs. 1 and 3a, are presented in Fig. 3b.

3. Comparison with other published results

a. Comparison with other estimates

In an analysis of the JONSWAP results, Hasselmann et al. (1973) suggested that the ratio of C_v/C_{10} was about 0.2 and might be higher at short fetches. For prevailing conditions of their experiments at nondimensional fetches of 10^3–10^4 and intermediate wind velocities around 10 m s^{-1}, the value suggested by them compares

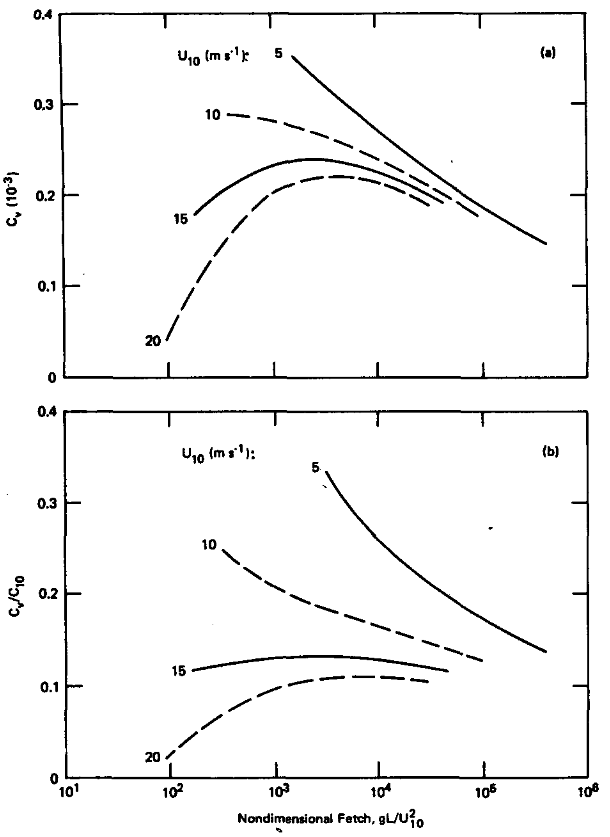

FIG. 3. Wave-drag coefficients and ratios between wave-drag and wind-stress coefficients at various nondimensional fetches.

well with the present estimate. We, however, have provided a much more detailed estimate to include variations of C_v/C_{10} with both wind velocity and fetch. The ratio for low and intermediate winds is indeed higher as suggested by Hasselmann et al., but lower at high winds.

Following his suggested scheme, Phillips (1977) also made a numerical estimate. The integration limits from the wave components at the spectral peak to where $c = 5u_*$ were approximated by $c = U_{10}$ and $0.25U_{10}$, respectively; in addition, a constant wind-stress coefficient of 1.5×10^{-3} was used. The value of his estimate, $C_v/C_{10} = 0.23$, aiming for open-sea conditions is greater than the present results.

b. Comparison with field measurements

Microscale fluctuations of the atmospheric pressure above surface gravity waves were measured in the field by Snyder et al. (1981). The fraction of momentum flux from wind directly to waves was reported to vary with the wind velocity (Fig. 4). Their experiments were extended over a long period of time with winds coming from all directions; the fetch for the results shown in Fig. 4 was unspecified. The fraction, however, is seen in the figure to increase with wind velocity from a value of about 0.3 at 4 m s^{-1} to about 0.8 at 7 m s^{-1}. It is hard to compare the measurements of Snyder et al. with our estimate without knowing the fetch. Nonetheless, encouraging similarities are illustrated between the results presented in Figs. 3b and 4, as the estimated ratio of C_v/C_{10} at low winds, say, around 5 m s^{-1}, increases sharply with wind velocity, and the estimated and measured values have a comparable range of variations.

4. Concluding remarks

Taking together reported variations of the wind stress and ocean waves with the nondimensional fetch, we have estimated the momentum flux from wind to long waves. The results are consistent with previous estimates; the latter, however, have been much extended to include variations with both fetch and wind velocity. Our estimates were also shown to have similar trends with the field measurements obtained at different wind velocities.

Excluding the direct momentum flux to the wind, the remainder of the wind stress is considered effective in producing aqueous flows. For the open sea, it is about 85% of the wind stress but varies with the nondimensional fetch. It is considerably less at short fetches and low winds; the latter is also the most prevailing wind condition for the open sea. In summary, the total wind stress should not be used in any oceanic model even for open-sea conditions, and a much smaller fraction of the wind stress should be used for lakes and coastal regions.

Acknowledgments. This note was prepared following a stimulating discussion with my colleague Richard

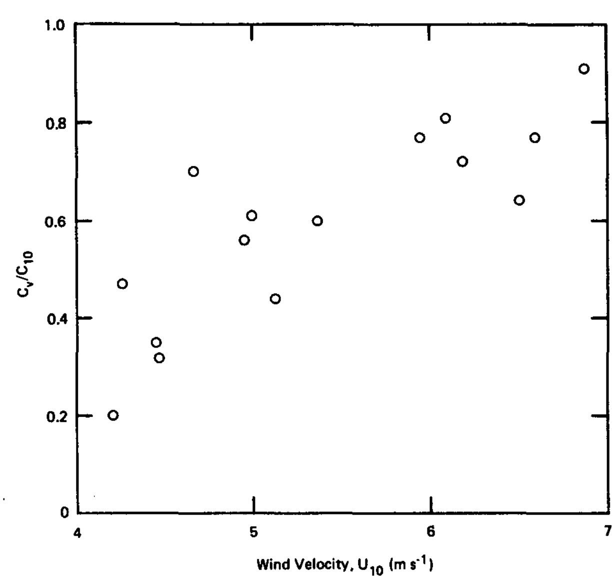

FIG. 4. Field measurements of C_v/C_{10} at various wind velocities (Snyder et al., 1981).

W. Garvine. The sponsorship of my work has been graciously provided by the Fluid Dynamics Program, Office of Naval Research under Contract N00014-83-K-0316.

REFERENCES

Burling, R. W., 1959: The spectrum of waves at short fetches. *Dtsch. Hydrogr. Z.*, **12**, 45–117.

Hasselmann, K., et al., 1973: Measurements of wind wave growth and swell decay during the Joint North Sea Wave Project, (JONSWAP). Reihe A (8°), Nr. 12, Deutsches Hydrographisches Institut, Hamburg.

Hicks, B. L., 1960: The energy spectrum of small wind waves. C.S.L. Rep. M-92, University of Illinois.

Kinsman, B., 1960: *Wind Waves*, Prentice-Hall, 676 pp.

Leykin, I. A., and A. D. Rozenberg, 1984: Sea-tower measurements of wind-wave spectra in the Caspian Sea. *J. Phys. Oceanogr.*, **14**, 168–176.

Lui, P. C., 1970: Normalized and equilibrium spectra of wind waves on Lake Michigan. *J. Phys. Oceanogr.*, **1**, 151–159.

Mitsuyasu, H., 1985: A note on momentum transfer from wind to waves. *J. Geophys. Res.*, **90**, 3343–3345.

Phillips, O. M., 1958: The equilibrium range in the spectrum of wind-generated waves. *J. Fluid Mech.*, **4**, 426–434.

——, 1977: *The Dynamics of the Upper Ocean*, 2nd ed., Cambridge University Press, 336 pp.

——, 1985: Spectral and statistical properties of the equilibrium range in wind-generated gravity waves. *J. Fluid Mech.*, **156**, 505–531.

Stewart, R. W., 1961: The wave drag of wind over water. *J. Fluid Mech.*, **10**, 189–194.

Snyder, R. L., F. W. Dobson, J. A. Elliott and R. B. Long, 1981: Array measurements of atmospheric pressure fluctuations above surface gravity waves. *J. Fluid Mech.*, **102**, 1–59.

Wu, Jin, 1971: Anemometer height in Froude scaling of wind stress. *J. Waterway, Harbors, Coastal Eng. Div.*, ASCE **98**, 963–975.

——, 1980: Wind-stress coefficients over sea surface near neutral conditions—a revisit. *J. Phys. Oceanogr.*, **10**, 727–740.

——, 1985: Parameterization of wind-stress coefficients over water surface. *J. Geophys. Res.*, **90**, 9069–9072.